The Probability Distribution of Sea Surface Wind Speeds. Part II: Dataset Intercomparison and Seasonal Variability

Adam Hugh Monahan

School of Earth and Ocean Sciences, University of Victoria, Victoria, British Columbia, and Earth System Evolution Program, Canadian Institute for Advanced Research, Toronto, Ontario, Canada

ABSTRACT

The statistical structure of sea surface wind speeds is considered, both in terms of the leading-order moments (mean, standard deviation, and skewness) and in terms of the parameters of a best-fit Weibull distribution. An intercomparison is made of the statistical structure of sea surface wind speed data from four different datasets: SeaWinds scatterometer observations, a blend of Special Sensor Microwave Imager (SSM/I) satellite observations with ECMWF analyses, and two reanalysis products [NCEP–NCAR and 40-yr ECMWF Re-Analysis (ERA-40)]. It is found that while the details of the statistical structure of sea surface wind speeds differs between the datasets, the leading-order features of the distributions are consistent. In particular, it is found in all datasets that the skewness of the wind speed is a concave upward function of the ratio of the mean wind speed to its standard deviation, such that the skewness is positive where the ratio is relatively small (such as over the extratropical Northern Hemisphere), the skewness is close to zero where the ratio is intermediate (such as the Southern Ocean), and the skewness is negative where the ratio is relatively large (such as the equatorward flank of the subtropical highs). This relationship between moments is also found in buoy observations of sea surface winds. In addition, the seasonal evolution of the probability distribution of sea surface wind speeds is characterized. It is found that the statistical structure on seasonal time scales shares the relationships between moments characteristic of the year-round data. Furthermore, the seasonal data are shown to depart from Weibull behavior in the same fashion as the year-round data, indicating that non-Weibull structure in the year-round data does not arise due to seasonal nonstationarity in the parameters of a strictly Weibull time series.

1. Introduction

Interactions between the ocean and atmosphere are strongly influenced by the probability distribution of sea surface wind speeds. Air–sea fluxes of momentum, energy, and material substances are generally found to have a nonlinear dependence on sea surface wind speed (e.g., Jones and Toba 2001; Donelan et al. 2002), so average fluxes depend not only on the average wind speed, but also on higher-order moments of the distribution. In consequence, the accurate characterization of the probability distribution of sea surface wind speeds is an important problem of meteorological, oceanographic, and climatic significance (e.g., Wright and Thompson 1983; Thompson et al. 1983; Isemer and

Hasse 1991; Wanninkhof 1992; Wanninkhof and McGillis 1999; Wanninkhof et al. 2002). It has been known for some time that the variability of sea surface wind speeds can be characterized to a good approximation by the two-parameter Weibull distribution (e.g., Pavia and O'Brien 1986; Erickson and Taylor 1989; Bauer 1996), although it has been stressed that this approximation is not exact (e.g., Tuller and Brett 1984; Erickson and Taylor 1989; Bauer 1996). A limitation of most of these earlier studies was the lack of high-resolution (in both space and time) records of sea surface wind speeds of sufficient duration to accurately characterize the distributions on a global scale. For example, the study of Pavia and O'Brien (1986) employed ship data from a single year, with poor spatial resolution outside of the extratropical Northern Hemisphere (NH). Conversely, the study of Isemer and Hasse (1991) made use of 30 yr of ship data but considered only the North Atlantic Ocean.

Over the last decade, unprecedentedly long time se-

Corresponding author address: Dr. Adam Hugh Monahan, School of Earth and Ocean Sciences, University of Victoria, P.O. Box 3055 STN CSC, Victoria, BC V8P 5C2, Canada.
E-mail: monahana@uvic.ca

ries of sea surface wind speeds with global coverage have become available from two primary sources: reanalysis products and satellite-derived remotely sensed observations. Reanalyses combine meteorological observations with full atmospheric general circulation models (GCMs) to find model states that are optimally compatible with the observations; the resulting datasets are of long duration, with high resolution in both space and time (e.g., Kalnay et al. 1996; Simmons and Gibson 2000). The reanalysis GCM, however, is only an approximate representation of the real atmosphere. Consequently, reanalysis products have the drawback that they will be corrupted by model biases, especially in poorly sampled regions where the reanalysis data reflect the model more than the observations. On the other hand, remotely sensed sea surface wind speeds have the benefit of being more direct measurements of sea surface winds and are generally found to agree reasonably well with in situ buoy and ship-based observations (e.g., Meissner et al. 2001; Ebuchi et al. 2002; Bourassa et al. 2003), but they are generally of limited duration (e.g., Kelly 2004). Buoy data represent real in situ observations, but their spatial coverage is limited, particularly in the open ocean. Because they are not corrupted by GCM biases, satellite observations of sea surface winds are preferred for applications that do not require long time series (e.g., Chelton et al. 2004); other applications, such as global estimates of air–sea fluxes (Wanninkhof et al. 2002), require the long datasets that are only available through reanalysis products. An intercomparison of the characterization of the probability distribution of sea surface wind speeds in different datasets is therefore a useful exercise.

Part I of the present study (Monahan 2006, hereafter Part I) characterized the statistical structure of the probability distribution of sea surface wind speeds, w, using 6 yr of daily vector wind data from the SeaWinds scatterometer mounted on the Quick Scatterometer (QuikSCAT) satellite. This characterization was in terms of both the leading few moments (mean, standard deviation, and skewness) as well as the parameters of the Weibull distribution. It was confirmed that the Weibull distribution is a good approximation to the distribution of sea surface wind speeds. In particular, both the SeaWinds observations and the Weibull distribution share the feature that the skewness of w is a concave upward function of the ratio of the mean of w to its standard deviation, such that the skewness is positive when the ratio is small, the skewness is near to zero when the ratio is intermediate, and the skewness is negative when the ratio is large. Using a simple stochastic model derived using a clear sequence of approximations from the boundary layer momentum equations, it

was shown that this relationship between moments is a consequence of the non-Gaussian structure of the sea surface vector winds resulting from the nonlinear dependence of surface drag on wind speed (Monahan 2004a,b).

Despite being well-approximated by a Weibull distribution, the SeaWinds observations were found to display distinct non-Weibull behavior. In particular, the slope of the relationship between mean(w)/std(w) and skew(w) was found to be steeper than the Weibull curve for low values of the ratio, and shallower than the Weibull curve for larger values. In geographical terms, the skewness of the observed wind speeds tends to be more negative in the Tropics, and more positive in the extratropics, than the equivalent Weibull variable. It was concluded, based on a Monte Carlo analysis, that the probability was vanishingly small of this non-Weibull structure arising because of sampling fluctuations of an underlying Weibull population. Spurious non-Weibull structure in observations of truly Weibull winds could arise for two further reasons: 1) biases in the data and 2) nonstationarities associated with the seasonal evolution of sea surface winds. As Part I of this study considered only data from the single SeaWinds dataset throughout the entire year, neither of these possibilities were assessed in detail.

The present study presents an intercomparison of the statistical structure of sea surface wind speeds in remotely sensed, reanalysis, and buoy wind datasets. In particular, this study considers the extent to which the relationships between the moments of sea surface wind speeds observed in the SeaWinds data characterize other sea surface wind datasets. Furthermore, we will investigate the variability of the probability distribution of sea surface wind speeds over the course of the seasonal cycle. The evolution of the moments and Weibull parameters of sea surface winds over the seasonal cycle will be documented, and the possibility that the non-Weibull structure observed in the SeaWinds sea surface wind data arises because of seasonal nonstationarities will be addressed.

A brief review of the properties of the Weibull distribution is presented in section 2, followed by an overview of the datasets considered in this study in section 3. An intercomparison of the statistical structure of the sea surface wind in the different datasets is presented in section 4, and a characterization of the seasonal evolution of the probability distributions is given in 5. A discussion and conclusions follow in section 6.

2. Statistical preliminaries

We will present a brief overview of the essential features of the Weibull distribution, a more thorough re-

view of which is presented in Part I of this study. A random variable x characterized by a two-parameter Weibull distribution has the probability density function (PDF)

$$p(x) = \frac{b}{a}\left(\frac{x}{a}\right)^{b-1}\exp\left[-\left(\frac{x}{a}\right)^{b}\right].\quad(1)$$

The parameters a and b denote, respectively, the scale and shape parameters. The averages of powers of x are given simply by

$$\text{mean}(x^{k}) = a^{k}\Gamma\left(1 + \frac{k}{b}\right),\quad(2)$$

where Γ is the gamma function. Expressions for the moments of x follow from Eq. (2). In particular, both the mean and standard deviation of x [denoted, respectively, mean(x) and std(x)] depend on both the a and b parameters, although the dependence of mean(x) on b is weak. On the other hand, the skewness and kurtosis of x, respectively, the normalized third- and fourth-order moments,

$$\text{skew}(x) = \frac{\text{mean}\{[x - \text{mean}(x)]^{3}\}}{\text{std}^{3}(x)}\quad(3)$$

$$= \frac{\Gamma\left(1 + \frac{3}{b}\right) - 3\Gamma\left(1 + \frac{1}{b}\right)\Gamma\left(1 + \frac{2}{b}\right) + 2\Gamma^{3}\left(1 + \frac{1}{b}\right)}{\left[\Gamma\left(1 + \frac{2}{b}\right) - \Gamma^{2}\left(1 + \frac{1}{b}\right)\right]^{3/2}},\quad(4)$$

$$\text{kurt}(x) = \frac{\text{mean}\{[x - \text{mean}(x)]^{4}\}}{\text{std}^{4}(x)} - 3\quad(5)$$

$$= \frac{\Gamma\left(1 + \frac{4}{b}\right) - 4\Gamma\left(1 + \frac{3}{b}\right)\Gamma\left(1 + \frac{1}{b}\right) + 6\Gamma\left(1 + \frac{2}{b}\right)\Gamma^{2}\left(1 + \frac{1}{b}\right) - 3\Gamma^{4}\left(1 + \frac{1}{b}\right)}{\left[\Gamma\left(1 + \frac{2}{b}\right) - \Gamma^{2}\left(1 + \frac{1}{b}\right)\right]^{2}} - 3,\quad(6)$$

depend only on the parameter b.

As is discussed in Part I, a number of different estimators of the Weibull parameters exist. In practice, it is found that differences in wind speed scale and shape parameters obtained from these different estimators are negligible. Therefore, we will use the simplest of these estimators:

$$a = \frac{\text{mean}(x)}{\Gamma(1 + 1/b)}\quad(7)$$

$$b = \left[\frac{\text{mean}(x)}{\text{std}(x)}\right]^{1.086}.\quad(8)$$

Note that the Weibull shape parameter b is uniquely determined by the ratio of mean(x) to std(x).

3. Data

The following datasets are considered in this study.

1) Daily level 3.0 gridded SeaWinds scatterometer 10-m zonal and meridional wind observations from the National Aeronautics and Space Administration (NASA) QuikSCAT satellite (Jet Propulsion Labo-

ratory 2001), available on a 1/4° × 1/4° grid from 19 July 1999 to the present (15 March 2005 for the present study). These data are available for download from the NASA Jet Propulsion Laboratory (JPL) Distributed Active Archive Center (see http://podaac.jpl.nasa.gov). The SeaWinds data have been extensively compared with buoy and ship measurements of surface winds (Ebuchi et al. 2002; Bourassa et al. 2003; Chelton and Freilich 2005); the root-mean-square errors of the remotely sensed wind speed and direction are both found to be dependent on wind speed, with average values of ~1 m s^{-1} and ~20° respectively. Because raindrops are effective scatterers of microwaves in the wavelength band observed by SeaWinds, rainfall can lead to errors in estimates of sea surface winds. The SeaWinds level 3.0 dataset flags those data points that are estimated as likely to have been corrupted by rain (Jet Propulsion Laboratory 2001); these data points have been excluded from the present analysis.

2) Six-hourly level 3.0 Special Sensor Microwave Imager (SSM/I) 10-m zonal and meridional wind data, variationally blending raw SSM/I retrievals with European Centre for Medium-Range Weather
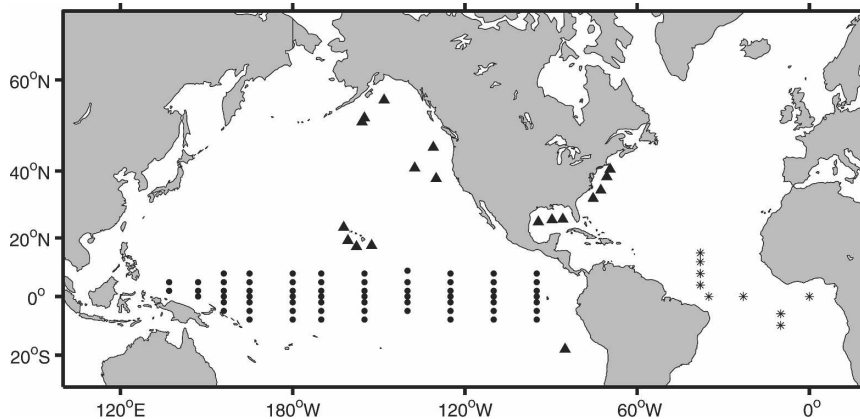
FIG. 1. Locations of buoys considered in this study (NDBC buoys: triangles; TAO buoys: filled circles; PIRATA buoys: asterisks).

Forecasts (ECMWF) analyses and in situ observations, available on a $1° \times 1°$ grid from 1 July 1987 to 31 December 2001. The dataset and blending algorithm are described in Atlas et al. (1996) and Meissner et al. (2001). These data are available from the NASA JPL Distributed Active Archive Center (see http://podaac.jpl.nasa.gov).

3) Six-hourly 40-yr ECMWF Re-Analysis (ERA-40) reanalysis 10-m zonal and meridional winds, available on a $2.5° \times 2.5°$ grid from 1 September 1957 to 31 August 2002 (Simmons and Gibson 2000). These data are available online (see http://data.ecmwf.int/data/d/era40/).

4) Six-hourly National Centers for Environmental Precipitation–National Center for Atmospheric Research (NCEP–NCAR) reanalysis 10-m zonal and meridional winds, available on a $1.875° \times 1.9°$ Gaussian grid from 1 January 1948 to 31 December 2002 (Kalnay et al. 1996). These data are available from the National Ocean and Atmospheric Administration–Cooperative Institute for Research in Environmental Sciences (NOAA–CIRES) Climate Diagnostics Center (see http://www.cdc.noaa.gov/).

5) Daily buoy observations obtained from the National Data Buoy Center (NDBC; data available from http://www.ndbc.noaa.gov) and from the Tropical Atmosphere–Ocean (TAO) and the Pilot Research Moored Array in the Tropical Atlantic (PIRATA) arrays (data available from the TAO Project Office, http://www.pmel.noaa.gov/tao/data_deliv/). The selected buoys (18 from NDBC, 66 from TAO, and 9 from PIRATA) each have a minimum of 730 days of observations and are sufficiently far from land that local coastal effects are minimal. For each buoy, sea surface temperature and surface atmosphere temperature were available, so the wind speed at the anemometer height was converted to 10-m wind speed using the stability-dependent method described in Liu and Tang (1996). The locations of these buoys are illustrated in Fig. 1.

No preprocessing, such as filtering or removing the annual cycle, was carried out on any of these datasets.

4. Sea surface wind dataset intercomparison

The wind speed datasets considered in this study are not mutually independent. The SSM/I dataset is a blend of satellite observations, ECMWF analysis fields, and some buoy observations. The model physics used in the preparation of these analysis fields will share essential features with the model physics used in the preparation of the reanalysis products. Furthermore, TAO buoy observations were assimilated into the ERA-40 product, and raw SSM/I surface wind speed estimates were assimilated into both the ERA-40 and NCEP–NCAR reanalysis. However, as noted in Meissner et al. (2001), for the NCEP–NCAR dataset SSM/I surface winds were estimated using an algorithm in accordance with Krasnopolsky et al. (1995) rather than the Wentz (1997) algorithm used for the ERA-40 and blended SSM/I datasets. ERA-40 also assimilates surface wind data from the European Space Agency Earth Remote Sensing (ERS)-1 and -2 scatterometers. Therefore, while these datasets are not independent, they are distinct and an intercomparison is meaningful.

a. Moments

The mean, standard deviation, skewness, and kurtosis fields of w from the SeaWinds, SSM/I, ERA-40, and NCEP–NCAR reanalysis datasets are displayed in Fig. 2. The moment fields estimated from the four datasets
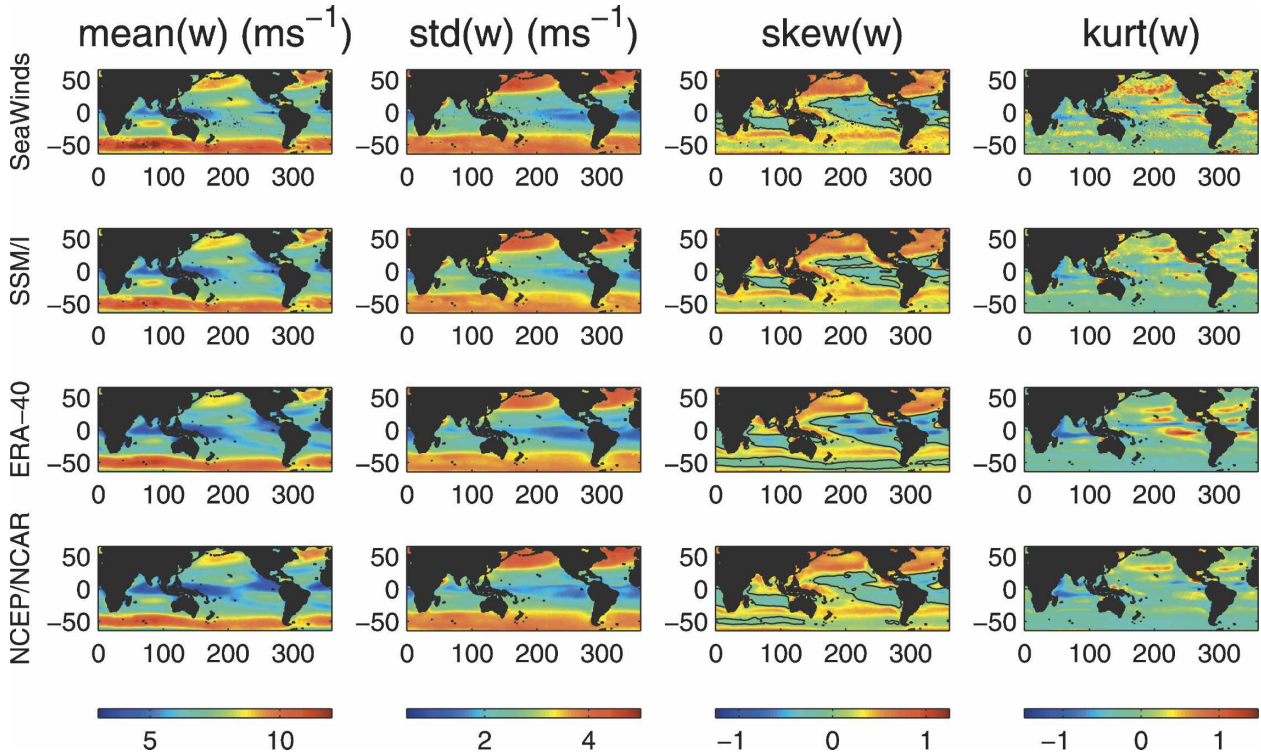
FIG. 2. Mean, std dev, skewness, and kurtosis fields for the SeaWinds, SSM/I, ERA-40, and NCEP–NCAR sea surface wind speed datasets. The solid line in the skewness plots is the zero contour.

share the same basic features. Maxima in mean(w) are evident over the Southern Ocean and in the NH midlatitude storm tracks. Secondary maxima of the mean wind speed are observed along the equatorward flanks of the subtropical high pressure cells, and minima are evident in the equatorial doldrums and subtropical horse latitudes. The standard deviation of w is largest in the midlatitude storm tracks and generally decreases equatorward; variability is generally smallest beneath the climatological subtropical anticyclones. A weak local maximum in std(w) lies along the intertropical convergence zone (ITCZ). The skewness of w is strongly positive in the NH extratropics and along the equatorward flank of the Southern Hemisphere (SH) westerly jet; it is close to zero over the Southern Ocean, and it is negative in those parts of the Tropics and subtropics characterized by strong and steady winds. The kurtosis of w is generally negative along the ITCZ and in the Indian Ocean, close to zero over the Southern Ocean and in much of the Tropics, and positive elsewhere.

While the moment fields estimated from the SeaWinds, SSM/I, ERA-40, and NCEP–NCAR datasets share the same basic features in common, they differ in details. Figure 3 presents maps of the SSM/I, ERA-40, and NCEP–NCAR moment fields minus the SeaWinds moment fields. It is evident that the SeaWinds mean(w)

field is generally larger than the mean(w) fields from the other datasets, although differences are small with mean(w) from SSM/I. Differences from the reanalysis datasets are particularly large in the Tropics and over the Southern Ocean. The SeaWinds std(w) field is slightly smaller than the SSM/I std(w) field in the Tropics and is slightly larger over the Southern Ocean. The ERA-40 std(w) is generally biased low relative to the SeaWinds std(w). Differences in std(w) between SeaWinds and the NCEP–NCAR reanalysis are typically small and spatially disorganized. The negative skew(w) in the Tropics is considerably weaker in the SSM/I and NCEP–NCAR datasets and slightly stronger in the ERA-40 dataset than in the SeaWinds observations. The ERA-40 skew(w) field is also more negative over the Southern Ocean than the skewness fields of the other datasets. Differences between kurt(w) fields estimated from the different datasets are larger than for the other moment fields. In general, the SeaWinds kurt(w) field is larger than the kurt(w) fields of the other datasets, although there are localized regions in which the sign of the difference is reversed.

Previous studies have noted that satellite observations of mean sea surface wind speeds tend to be larger than analysis or reanalysis estimates in both the Tropics (e.g., Meissner et al. 2001; Bentamy et al. 2003) and
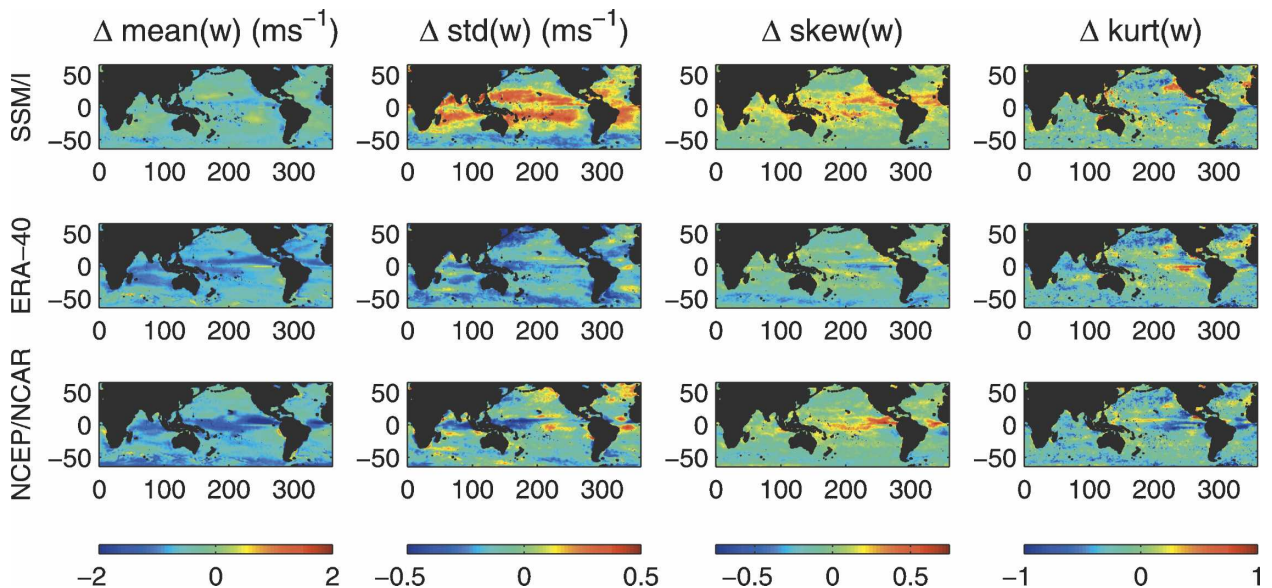
FIG. 3. Maps of the mean, std dev, skewness, and kurtosis fields of the SSM/I, ERA-40, and NCEP–NCAR datasets minus the corresponding fields of the SeaWinds observations.

over the Southern Ocean (e.g., Yuan 2004); these earlier results are consistent with the differences presented in Fig. 3. Caires et al. (2004) noted that mean(w) in the Tropics was higher in the ERA-40 data than in the NCEP–NCAR reanalysis data, again consistent with the results presented in Fig. 3. Chelton and Freilich (2005) compared SeaWinds wind speed observations with NCEP and ECMWF operational analysis fields and also found that in some years the ECMWF analysis mean(w) is biased low relative to the SeaWinds mean(w) field, although it is also biased low relative to the NCEP analyses.

As was noted by Chelton and Freilich (2005), some of the differences in mean(w) between the remotely sensed and reanalysis datasets may arise because satellite observations measure wind stress, which is then converted to 10-m equivalent neutral-stability winds without accounting for stratification effects (Liu and Tang 1996). Reanalysis models, on the other hand, attempt to simulate the actual winds at 10 m. Chelton and Freilich (2005) estimate that the difference between actual 10-m winds and equivalent neutral-stability winds can account for ~0.2 m s^{-1} of the difference between the remotely sensed and simulated wind fields. Furthermore, reanalysis models do not resolve small-scale structures in sea surface temperature that modify the local boundary layer stability with a measurable local effect on sea surface winds (e.g., Chelton et al. 2004). Chelton and Freilich (2005) also emphasize the fact that remotely sensed observations of sea surface winds are sensitive to the vector velocity difference between the

ocean surface and the 10-m wind, rather than the 10-m wind itself, while reanalysis models neglect surface currents and assume a rigid bottom boundary; reanalyzed wind fields will therefore be biased relative to remotely sensed winds in regions of swift surface currents (e.g., Kelly et al. 2001, 2005). This effect may account for some of the differences between the moment fields, particularly in the regions of relatively swift surface currents around the equator and the Southern Ocean.

b. Weibull parameters

Fields of the Weibull scale and shape parameters, a and b, for each of the SeaWinds, SSM/I, ERA-40, and NCEP–NCAR surface wind speed datasets are presented in Fig. 4. For each of the datasets considered, the field of the Weibull shape parameter a has essentially the same structure as the field of mean(w). Furthermore, all four datasets share the same overall distribution of b: the Weibull shape parameter varies between 2 and 3 in the NH midlatitudes, over the Indo-Pacific warm pool, and on the equatorward flank of the SH surface westerly jet; between 3 and 4 over the Southern Ocean; and above 4 on the equatorward flanks of the subtropical highs, with values up to 6 over the subtropical Atlantic and eastern Pacific. Maxima in b are generally larger in the SeaWinds and ERA-40 surface wind data than in the SSM/I and NCEP–NCAR reanalysis datasets.

As was discussed in Part I of this study, an essential feature shared by both the SeaWinds sea surface wind observations and the Weibull distribution is
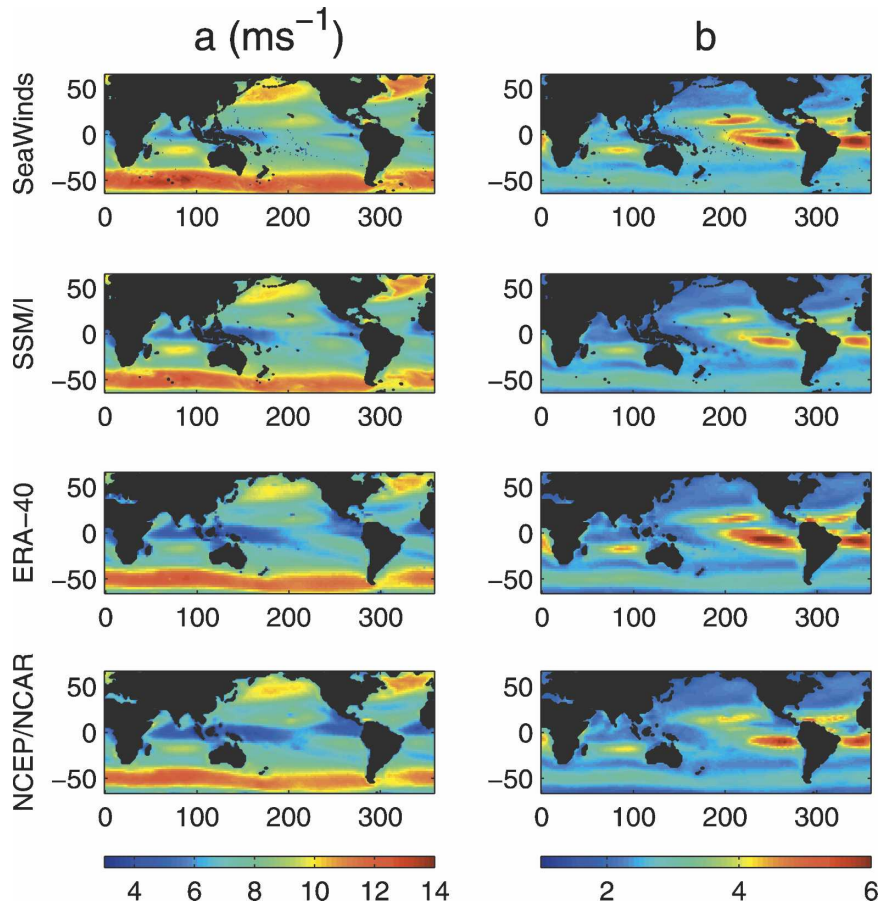
FIG. 4. Same as in Fig. 2, but for the Weibull *a* and *b* parameters.

that skew(w) is a concave upward function of the ratio mean(w)/std(w), such that the skewness is positive where the ratio is small, near zero where the ratio is intermediate, and negative where the ratio is large. Kernel density estimates of the joint PDF of mean(w)/std(w) with skew(w) for each of the SeaWinds, SSM/I, ERA-40, and NCEP–NCAR reanalysis datasets are presented in Fig. 5, along with the theoretical curve for a Weibull variable. A scatterplot of mean(w)/std(w) against skew(w) for the buoy data is presented in Fig. 6.
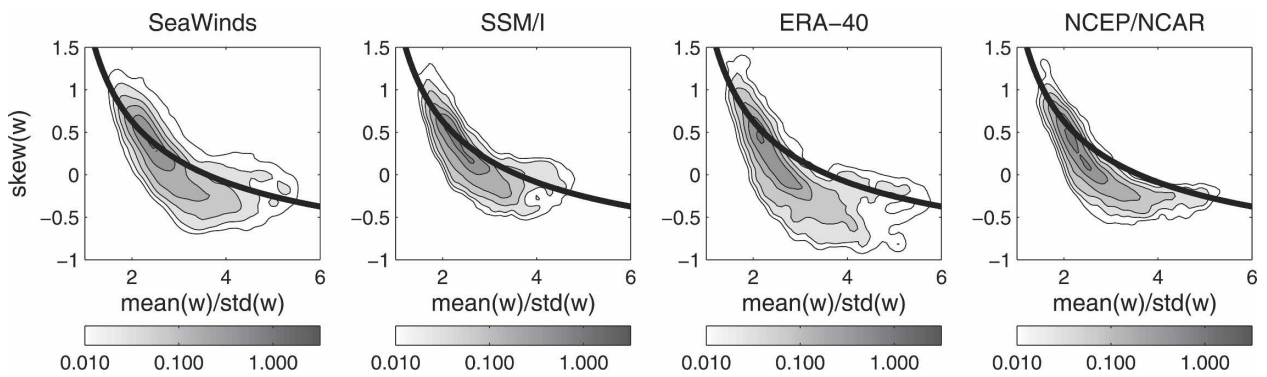

FIG. 5. Kernel density estimates of the joint PDFs (contoured on logarithmic scales) of mean(w)/std(w) with skew(w) for SeaWinds, SSM/I, ERA-40, and NCEP–NCAR sea surface wind speeds. The thick black curve is the predicted relationship between moments for a Weibull variable.
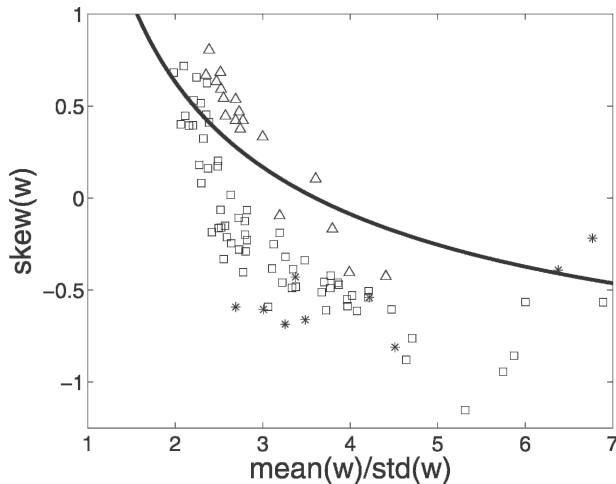
FIG. 6. Scatterplot of mean(w)/std(w) vs skew(w) for NDBC (triangles), TAO (squares), and PIRATA (asterisks) buoy observations. The solid curve is the predicted relationship between moments for a Weibull variable.

Too few buoys were available for a meaningful estimate to be made of the joint PDF of mean(w)/std(w) with skew(w) from buoy data. Evidently, despite differences in detail, all five datasets are in qualitative agreement regarding the relationship between the moments of sea surface wind speed. In particular, the theoretical Weibull curve runs through the joint PDFs of the Sea-Winds, SSM/I, ERA-40, and NCEP–NCAR reanalysis data, and through the scatter of the buoy data. It is demonstrated in Part I that the relationships between the fields of mean(w), std(w), and skew(w) can be qualitatively understood in terms of boundary layer dynamics subject to fluctuating large-scale forcing and nonlinear surface drag.

There is also agreement among these five datasets regarding deviations in the structure of wind speed PDFs from Weibull. In all datasets, the slope of the relationship between skew(w) and the ratio mean(w)/std(w) is steeper than that of the Weibull curve for low values of the ratio, and it is shallower than that of the Weibull curve for larger values of the ratio. Using a Monte Carlo approach, it was demonstrated in Part I that the probability was vanishingly small of the apparent non-Weibull structure of the SeaWinds observations arising due to sampling fluctuations of a truly Weibull population. Similar calculations for the SSM/I, ERA-40, NCEP–NCAR reanalysis, and buoy datasets (not shown) indicate that the probability is also vanishingly small such that the non-Weibull structure in these datasets is attributable to sampling fluctuations of a Weibull variable.

To examine the geographical distribution of non-

Weibull structure in sea surface winds, maps of the observed skew(w) field minus the skew(w) field predicted for a Weibull variable with the observed mean(w) and std(w) [Eq. (4)] were computed for each of the SeaWinds, SSM/I, ERA-40, and NCEP–NCAR datasets (Fig. 7). In all four datasets, the estimated skew(w) is more negative in the Tropics and more positive in the NH midlatitudes than is the skewness field for the equivalent Weibull variable. In the reanalysis datasets, the skewness field over the Southern Ocean is more negative than the skewness of the equivalent Weibull field; this is consistent with the negative biases in these datasets of skew(w) over the Southern Ocean evident in Figs. 2 and 3.
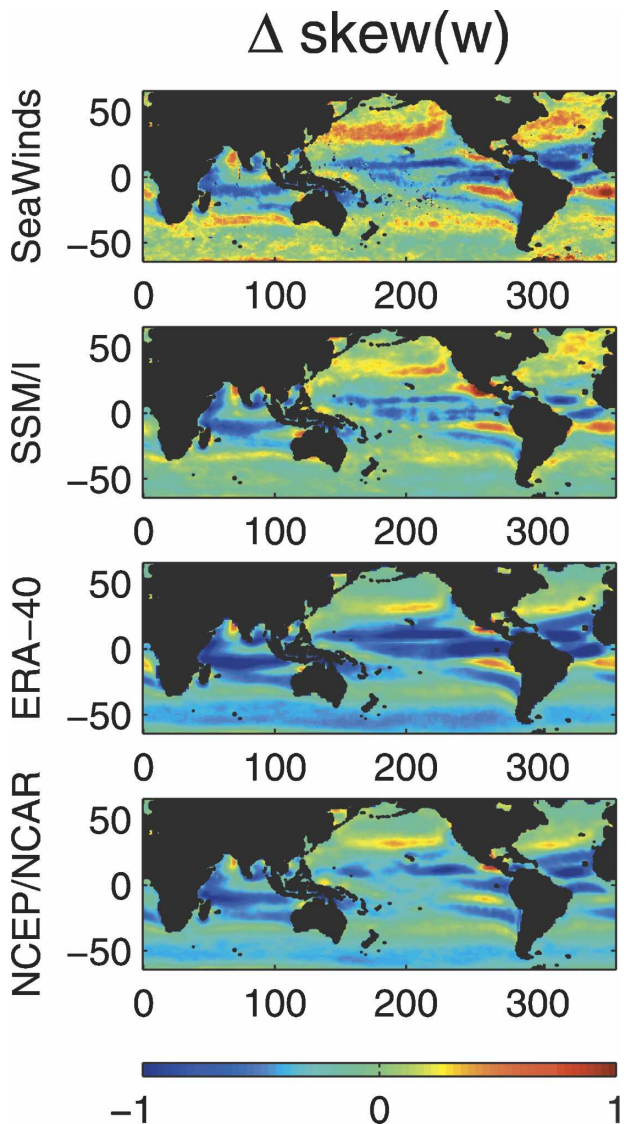

FIG. 7. Maps of the observed SeaWinds, SSM/I, ERA-40, and NCEP–NCAR skew(w) fields minus the skew(w) fields of the equivalent Weibull variables.
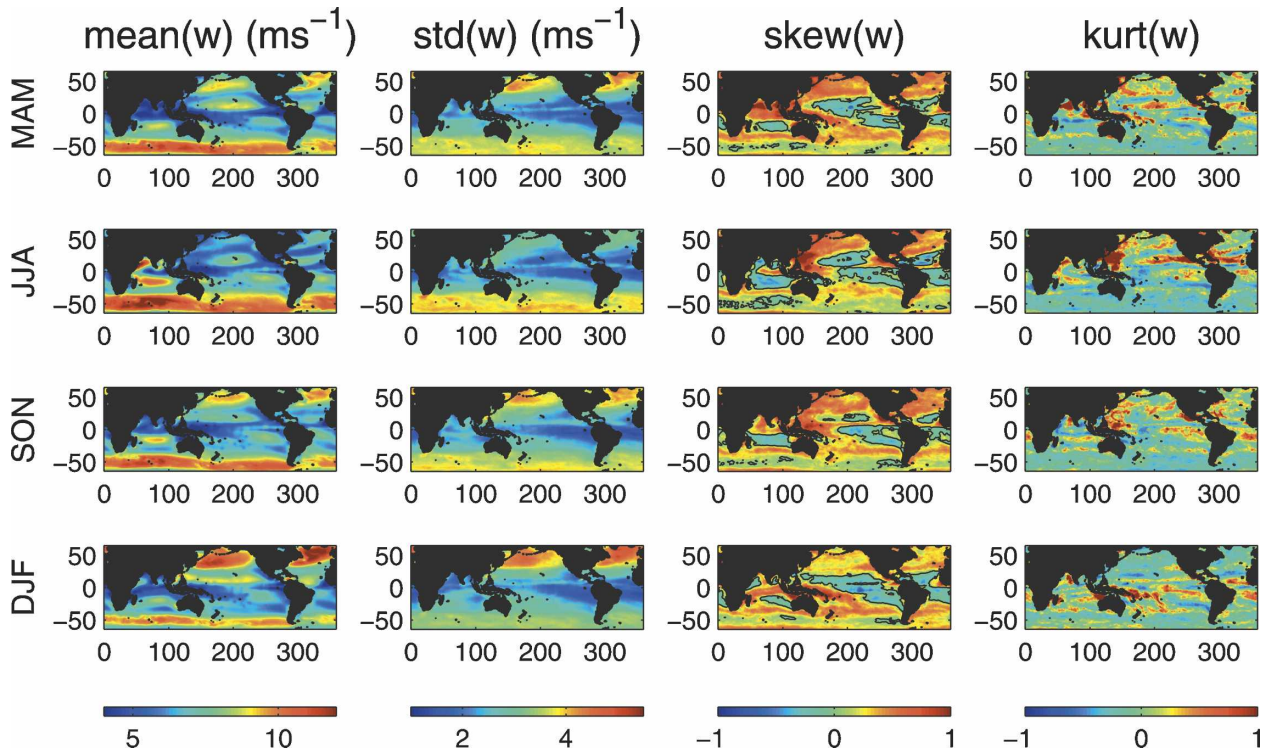
FIG. 8. Same as in Fig. 2, but for each of the MAM, JJA, SON, and DJF seasons for the SSM/I data.

In Part I of this study, it was noted that the Weibull distribution provides a reasonable approximation to the PDF of SeaWinds sea surface wind speeds, although there are large-scale differences between the observed moment fields and those associated with best-fit Weibull distributions. The present analysis demonstrates that these differences are evident in all the datasets under consideration and that the main features of the differences between observed and Weibull moment fields are consistent between different datasets.

5. Seasonal variability

The analyses of the PDFs of sea surface wind speed presented in the previous section and in Part I used data from throughout the entire year, without regard for seasonal variability. Considerable regional (if not global) seasonal evolution of the PDF of w is expected. Characterization of this seasonal variability is a basic element of the full characterization of the PDF of sea surface wind speeds. Furthermore, it is possible that the apparent non-Weibull structure of the sea surface wind speeds discussed in the previous section is a consequence of this nonstationarity in the statistics of w: seasonal evolution in the a and b parameters of an instantaneously Weibull variable could yield a year-round

PDF that is no longer Weibull. To assess the seasonal evolution of the probability distributions of sea surface winds, the SSM/I dataset is subdivided into four seasons: March–May (MAM); June–August (JJA); September–November (SON), and December–February (DJF). The SSM/I dataset is used rather than the SeaWinds observations because of its relatively long duration; as was discussed in section 4, the PDFs of sea surface wind speed in the SeaWinds and SSM/I datasets agree in their essential features. A description follows of the seasonal evolution of the statistical properties of w, in terms of both moments and Weibull parameters.

a. Moments

The fields of mean(w), std(w), skew(w), and kurt(w) for each of the MAM, JJA, SON, and DJF seasons are presented in Fig. 8. The seasonal cycle in mean(w) is greatest in the midlatitudes, particularly in the Northern Hemisphere, with the strongest mean wind speeds occurring in the winter season (DJF in NH; JJA in SH). Annual variability in mean(w) is considerably smaller in the subtropics, with somewhat stronger mean wind speeds along the equatorward flank of the subtropical highs in the winter season than in the summer. An exception in the subtropics is the equatorward flank of the Indian Ocean subtropical high, which displays a
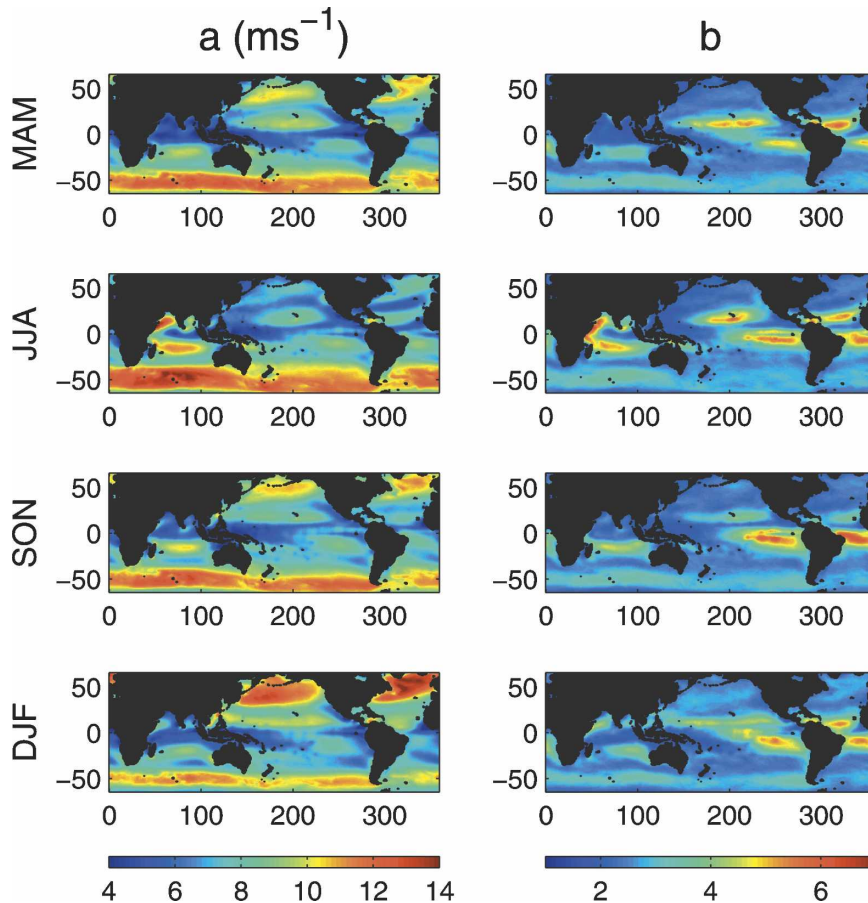
FIG. 9. Same as in Fig. 4, but for each of the MAM, JJA, SON, and DJF seasons for the SSM/I data.

marked annual cycle in mean(w) associated with the Australasian monsoon. A seasonal meridional migration of the equatorial doldrums is also evident.

As was the case with mean(w), midlatitude values of std(w) are stronger in the winter season than in the summer season, with a strong seasonal cycle evident in the NH and a weaker cycle in the SH. Variability in the subtropics is relatively weak in all seasons.

Throughout the seasonal cycle, skew(w) is positive in the NH extratropics; in general, largest positive values occur in JJA and smallest positive values occur in DJF. Conversely, skew(w) remains close to zero throughout the year over the Southern Ocean. The band of positive skewness on the equatorward flank of the SH surface westerly jet varies in strength over the seasonal cycle in opposite phase to the cycle of mean(w) in the jet: skew(w) in this band is relatively high when the mean jet is weak, and skew(w) is relatively low when the jet is strong. In the subtropics, the region in which skew(w) is negative evolves seasonally. Generally, in the summer (winter) hemisphere, this region is somewhat

larger (smaller) and the values of skew(w) are more (less) strongly negative. An exception to this tendency is in the subtropical Indian Ocean, in which skew(w) becomes most strongly negative on the equatorward flank of the subtropical high in the NH summer. Skewness of w is positive over the Indo-Pacific warm pool throughout the year. In general, the most negative values of kurt(w) in the extratropics of either hemisphere occur in the winter season and the most positive values occur in the summer season. In all seasons, the kurt(w) field is relatively noisy in comparison to the lower-order moment fields.

b. Weibull parameters

Fields of the Weibull size and shape parameters, a and b, for each of the MAM, JJA, SON, and DJF seasons are displayed in Fig. 9. The seasonal evolution of a follows that of mean(w), as would be expected. Throughout the seasonal cycle, values of b are between 2 and 3 in the NH extratropics, over the Indo-Pacific warm pool, and along the equatorward flank of the SH
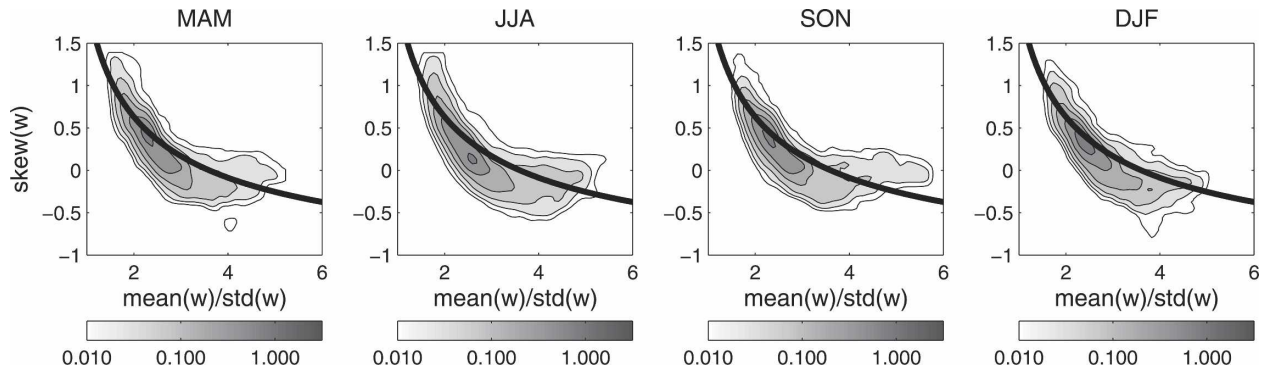
FIG. 10. Same as in Fig. 5, but for each of the MAM, JJA, SON, and DJF seasons of the SSM/I data.

westerly jet. Over the Southern Ocean, b varies between 3 and 4. In all seasons, the largest values of b occur in the subtropics, along the equatorward flanks of the subtropical highs where mean(w) is strong and std(w) is relatively low; in these regions, b can exceed a value of 5. In general, b is largest in the spring and summer.

January and July maps of the Weibull b parameter in the North Atlantic sector estimated from 30 yr worth of ship data were presented in Isemer and Hasse (1991). This earlier study indicated that b is close to 2 throughout the North Atlantic with the exception of a subtropical band of high values (between 3 and 4) that migrated equatorward in the winter and poleward in the summer, in close agreement with the seasonal evolution of b displayed in Fig. 9. Conversely, the results of Pavia and O'Brien (1986, hereafter PO) differ significantly from the results of the present study. Pavia and O'Brien considered a single year of ship observations, zonally averaged into four different ocean basins (Atlantic, Indian, western Pacific, and eastern Pacific). As is discussed in Part I, the data coverage in PO of the Tropics and SH midlatitudes was sparse. The annual cycles of the Weibull-scale parameter a reported in PO are broadly in agreement with the results presented in Fig. 9. On the other hand, the estimates of b presented in PO are markedly different than those of the present study. The values of b reported in PO are in general considerably lower than those presented in Fig. 9; in particular, the results of PO present no evidence over any of the four ocean basins of subtropical maxima in b. These maxima appear in all datasets considered in this study and in all seasons, and their existence is consistent with the regions of negatively skewed w described in this study and in Bauer (1996). We conclude that the differences between the characterization of b in PO and that of the present study, both in terms of geographical structure and seasonal evolution, arise because of the limited data used in PO (leading to sampling errors)

and their use of zonal averaging (as structure in b is not zonally symmetric).

To assess whether the apparent non-Weibull structure of w evident in Figs. 5–7 is a result of seasonal variation in the Weibull parameters, the joint PDFs of mean(w)/std(w) with skew(w) were calculated for each of the MAM, JJA, SON, and DJF seasons (Fig. 10). For each season, the joint PDF is characterized by the relationship between moments characteristic of the full year (Fig. 5), such that the theoretical curve for a Weibull variable runs through the joint PDF. Evidently, the seasonal sea surface wind speeds are no less Weibull than the full-year wind speeds. However, neither are they more Weibull: as in the year-round data, for each season the slope of the relationship between the ratio mean(w)/std(w) and skew(w) is steeper than the slope of the Weibull curve for small values of the ratio and shallower for large values of the ratio. The non-Weibull structure characteristic of the full-year data is also evident in the seasonally stratified data.

Maps of the SSM/I skew(w) field minus the equivalent Weibull skew(w) field obtained using the SSM/I mean(w) and std(w) fields, for each of the MAM, JJA, SON, and DJF seasons, are presented in Fig. 11. In all seasons, difference fields between the observed and Weibull fields are similar in pattern and magnitude to difference fields obtained using data from throughout the year (the second panel in Fig. 7). Evidently, the deviation of the year-round PDF of w from Weibull is not a consequence of seasonal nonstationarity: the sea surface wind speeds in each season also display considerable non-Weibull behavior.

6. Discussion and conclusions

A number of previous studies (e.g., PO; Isemer and Hasse 1991; Bauer 1996; Pryor and Barthelmie 2002) have investigated the probability distribution of sea surface wind speeds, w, in which it has been demonstrated
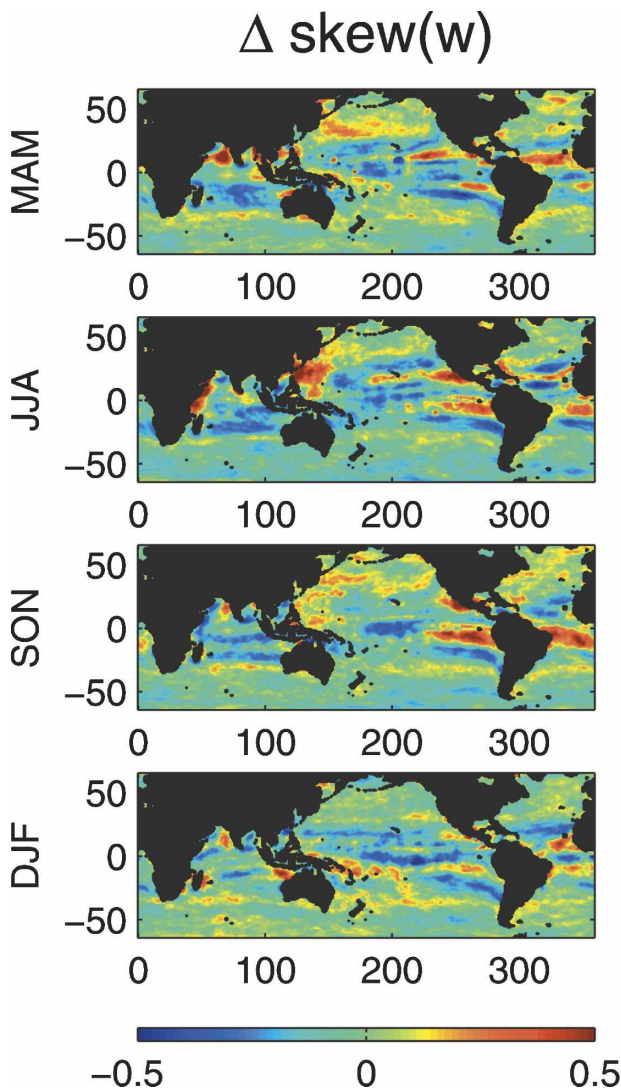
Δ skew(w)

Fig. 11. Same as in Fig. 7, but for each of the MAM, JJA, SON, and DJF seasons for the SSM/I data.

these datasets are reanalysis products (NCEP–NCAR and ERA-40) obtained by using an atmospheric general circulation model to dynamically interpolate between observations that are unevenly sampled in space and time. A third dataset, the SSM/I, is derived from passive satellite observations of the sea surface blended with surface analysis fields to fill in data gaps and provide wind directions. A fourth dataset consists of active sea surface vector wind observations from the SeaWinds scatterometer on the QuikSCAT satellite. A significant drawback of the first three of these datasets is that they are hybrids of observations and models, but they have the benefit of being of relatively long duration. Conversely, the scatterometer sea surface wind speeds are more direct observations, but presently only 6 yr of data are available. Importantly, these datasets agree (in essential features) in their characterization of the probability density functions of sea surface wind speeds, both in terms of the three lowest-order moments and of the best-fit parameters to the Weibull distribution. In particular, in all datasets considered, the wind speed skewness field has been shown to have a characteristic functional dependence on the ratio of the mean of the wind speed to its standard deviation: the skewness is a concave upward function of this ratio, such that it is positive for small values of the ratio, near zero for intermediate values, and negative for larger values. This relationship was also shown to hold in buoy data from the Northern Hemisphere midlatitudes and the tropical Pacific and Atlantic Oceans. The Weibull distribution has been shown to provide a reasonably accurate approximation to this relationship, although distinctly non-Weibull behavior is evident in all datasets.

It should be noted, however, that the quantitative differences between the PDFs of w characterized by the different datasets considered in this study are not negligible. Quantities such as air–sea fluxes estimated using these different datasets will thus differ quantitatively. Because they are not corrupted by GCM biases, Sea-Winds observations would generally be preferred for such calculations. However, some applications, such as global estimates of air–sea fluxes (e.g., Isemer and Hasse 1991; Wanninkhof et al. 2002) over long time scales, require the long datasets that are only available through reanalysis products. The biases of the wind speed moments in the different datasets described in the present study should be taken into account when interpreting the results of calculations in which these wind speed datasets have been used.

The present study has also considered the evolution of the PDFs of sea surface wind speeds over the annual

that the probability distribution is generally well approximated by the two-parameter Weibull distribution. However, most of these earlier studies were regional in scale. The one previous effort to characterize the probability distribution of w on a global scale (PO) used only a single year's data with limited coverage in the Tropics and the Southern Hemisphere. The recent development of global-scale wind speed datasets of several years' duration allows a reevaluation of the characterization of the probability distribution of sea surface wind speeds over the entire World Ocean.

In this study, an intercomparison has been made of the probability distribution of sea surface wind speeds as characterized by four global datasets of long duration with high resolution in space and time. Two of

cycle in the SSM/I dataset. It is found that the Weibull approximation is equally good in each of the MAM, JJA, SON, and DJF calendar seasons, and that the deviations from Weibull behavior evident in the full-year data are not simply a result of the seasonal nonstationarity of the Weibull parameters. The present study extends the result of previous studies characterizing the seasonal evolution of the sea surface wind speed Weibull parameters, which were geographically limited (e.g., Isemer and Hasse 1991) or used a dataset of too limited a duration to yield statistically robust estimates (e.g., PO).

The present study has taken advantage of long-duration global datasets of sea surface winds with high resolution in space and time that have only recently become available to produce a statistically robust characterization of the seasonal and geographical structure of the probability distribution of sea surface wind speeds. It is to be expected that refinements to this picture will be made as the quality and duration of wind speed datasets improve. Given the leading-order similarity of the statistical properties of the four datasets considered, however, it is not expected that the characterization of large-scale features in sea surface wind speed PDFS will change qualitatively. In particular, it is evident in all datasets and in all seasons that skew(w) is a concave upward function of the ratio mean(w)/std(w), positive where this ratio is small, close to zero where the ratio is intermediate, and negative where the ratio is large. A mechanistic model presented in Part I of this study is able to qualitatively characterize this relationship but is quantitatively inaccurate. A goal of future research will be the construction of physically based models that can quantitatively reproduce the robust relationships between statistical moments of the sea surface wind speeds that have been demonstrated in this study.

REFERENCES

Atlas, R., R. Hoffman, S. Bloom, J. Jusem, and J. Ardizzone, 1996: A multiyear global surface wind velocity dataset using SSM/I wind observations. *Bull. Amer. Meteor. Soc.,* **77,** 869–882.

Bauer, E., 1996: Characteristic frequency distributions of remotely sensed *in situ* and modelled wind speeds. *Int. J. Climatol.,* **16,** 1087–1102.

Bentamy, A., K. B. Datsaros, A. M. Mestas-Nuñez, W. M. Drennan, E. B. Forde, and H. Roquet, 2003: Satellite estimates of wind speed and latent heat flux over the global oceans. *J. Climate,* **16,** 637–656.

Bourassa, M. A., D. M. Legler, J. J. O'Brien, and S. R. Smith, 2003: SeaWinds validation with research vessels. *J. Geophys. Res.,* **108,** 3019, doi:10.1029/2001JC001028.

Caires, S., A. Sterl, J.-R. Bidlot, N. Graham, and V. Swail, 2004: Intercomparison of different wind–wave reanalyses. *J. Climate,* **17,** 1893–1912.

Chelton, D. B., and M. H. Freilich, 2005: Scatterometer-based assessment of 10-m wind analyses from the operational ECMWF and NCEP numerical weather prediction models. *Mon. Wea. Rev.,* **133,** 409–429.

——, M. G. Schlax, M. H. Freilich, and R. F. Milliff, 2004: Satellite measurements reveal persistent small-scale features in ocean winds. *Science,* **303,** 978–983.

Donelan, M., W. Drennan, E. Saltzman, and R. Wanninkhof, Eds., 2002: *Gas Transfer at Water Surfaces.* Amer. Geophys. Union, 383 pp.

Ebuchi, N., H. C. Graber, and M. J. Caruso, 2002: Evaluation of wind vectors observed by QuikSCAT/SeaWinds using ocean buoy data. *J. Atmos. Oceanic Technol.,* **19,** 2049–2062.

Erickson, D. J., and J. A. Taylor, 1989: Non-Weibull behavior observed in a model-generated global surface wind field frequency distribution. *J. Geophys. Res.,* **94,** 12 693–12 698.

Isemer, H., and L. Hasse, 1991: The scientific Beaufort equivalent scale: Effects on wind statistics and climatological air–sea flux estimates in the North Atlantic Ocean. *J. Climate,* **4,** 819–836.

Jet Propulsion Laboratory, cited 2001: SeaWinds on QuikSCAT Level 3: Daily, gridded ocean wind vectors. Tech. Rep. JPL PO.DAAC Product 109, California Institute of Technology. [Available online at http://podaac.jpl.nasa.gov:2031/DATASET_DOCS/qscat_L3.html.]

Jones, I. S., and Y. Toba, Eds., 2001: *Wind Stress over the Ocean.* Cambridge University Press, 307 pp.

Kalnay, E., and Coauthors, 1996: The NCEP/NCAR 40-Year Reanalysis Project. *Bull. Amer. Meteor. Soc.,* **77,** 437–471.

Kelly, K. A., 2004: Wind data: A promise in peril. *Science,* **303,** 962–963.

——, S. Dickinson, M. J. McPhaden, and G. C. Johnson, 2001: Ocean currents evident in ocean wind data. *Geophys. Res. Lett.,* **28,** 2469–2472.

——, ——, and G. C. Johnson, 2005: Comparisons of scatterometer and TAO winds reveal time-varying surface currents for the tropical Pacific Ocean. *J. Atmos. Oceanic Technol.,* **22,** 735–745.

Krasnopolsky, V., L. Breaker, and W. Gemmill, 1995: A neural network as a nonlinear transfer function model for retrieving surface wind speeds from the SSM/I. *J. Geophys. Res.,* **100,** 11 033–11 045.

Liu, W. T., and W. Tang, 1996: Equivalent neutral wind. Tech. Rep., JPL Publication 96-17, Pasadena, CA, 8 pp.

Meissner, T., D. Smith, and F. Wentz, 2001: A 10 year intercomparison between collocated Special Sensor Microwave Imager oceanic surface wind speed retrievals and global analyses. *J. Geophys. Res.,* **106,** 11 731–11 742.

Monahan, A. H., 2004a: Low-frequency variability of the statistical moments of sea-surface winds. *Geophys. Res. Lett.,* **31,** L10302, doi:10.1029/2004GL019599.

——, 2004b: A simple model for the skewness of global sea surface winds. *J. Atmos. Sci.,* **61,** 2037–2049.

——, 2006: The probability distribution of sea surface wind speeds. Part I: Theory and SeaWinds observations. *J. Climate,* **19,** 497–520.

Pavia, E. G., and J. J. O'Brien, 1986: Weibull statistics of wind speed over the ocean. *J. Climate Appl. Meteor.,* **25,** 1324–1332.

Pryor, S., and R. Barthelmie, 2002: Statistical analysis of flow characteristics in the coastal zone. *J. Wind Eng. Ind. Aerodyn.,* **90,** 201–221.

Simmons, A., and J. Gibson, 2000: The ERA-40 project plan. ERA-40 Project Rep. Series 1, ECMWF, Reading, United Kingdom, 63 pp.

Thompson, K., R. Marsden, and D. Wright, 1983: Estimation of low-frequency wind stress fluctuations over the open ocean. *J. Phys. Oceanogr.,* **13,** 1003–1011.

Tuller, S. E., and A. C. Brett, 1984: The characteristics of wind velocity that favor the fitting of a Weibull distribution in wind speed analysis. *J. Climate Appl. Meteor.,* **23,** 124–134.

Wanninkhof, R., 1992: Relationship between wind speed and gas exchange over the ocean. *J. Geophys. Res.,* **97,** 7373–7382.

——, and W. R. McGillis, 1999: A cubic relationship between air-sea CO_2 exchange and wind speed. *Geophys. Res. Lett.,* **26,** 1889–1892.

——, S. C. Doney, T. Takahashi, and W. R. McGillis, 2002: The effect of using time-averaged winds on regional air-sea CO_2 fluxes. *Gas Transfer at Water Surfaces,* M. A. Donelan et al., Eds., Amer. Geophys. Union, 351–356.

Wentz, F., 1997: A well-calibrated ocean algorithm for Special Sensor Microwave/Imager. *J. Geophys. Res.,* **102,** 8703–8718.

Wright, D. G., and K. R. Thompson, 1983: Time-averaged forms of the nonlinear stress law. *J. Phys. Oceanogr.,* **13,** 341–345.

Yuan, X., 2004: High-wind-speed evaluation in the Southern Ocean. *J. Geophys. Res.,* **109,** D13101, doi:10.1029/2003JD004179.